Influence of Fe/B ratio upon molybdenum tracer diffusion in crystallized Fe$_{79-y}$Mo$_8$Cu$_1$B$_{12+y}$ alloy

J. Čermák*, I. Stloukal

Institute of Physics of Materials, AS CR, Žižkova 22, CZ-61662 Brno, Czech Republic

Abstract

^{99}Mo tracer diffusion coefficient in Fe$_{79-y}$Mo$_8$Cu$_1$B$_{12+y}$ ($y = 0, 3, 5$) alloys was measured using serial sectioning method in the temperature range 573–773 K. The measurement was carried out with the ribbon-like samples crystallized before the diffusion experiment by a thermal shock in vacuum. The measured profiles were linear in co-ordinates ln c_{Mo} vs. $x^{1.5}$ (c_{Mo} – concentration of Mo in depth x), indicating that the diffusion of ^{99}Mo was controlled by "type A-B" kinetics.

K e y w o r d s: iron alloys, metallic glasses, diffusion

1. Introduction

Nanostructured materials are steadily in focus of interest in the last years. All stages of production of this family of materials [1–5] as well as study of their characteristics [6, 7] are open for further research. Behaviour of these materials depends on their internal structure, which is, in principle, thermodynamically unstable.

The iron-based amorphous or partly crystallized alloys are very prospective materials due to their advantageous magnetic characteristics. Iron-based materials containing molybdenum seem to be of extraordinary importance. Much effort has been devoted to optimization of their composition with respect to their glass forming ability, crystallization of magnetic phases and Curie temperature. Variation of Fe/B ratio in Fe-Mo-Cu-B alloys [8] led to a conclusion that the optimum composition may be somewhere close to Fe$_{76}$Mo$_8$Cu$_1$B$_{15}$, where the best glass formation was observed.

Since the rate of structural changes is – to a great extent – diffusion controlled, it is understood that the knowledge of diffusion kinetic parameters is of a substantial importance for the assessment of functional durability of final products.

In preceding paper [6] the diffusion of alloy components Fe and Mo was studied in as-received state and in relaxed structures of amorphous alloy Fe$_{76}$Mo$_8$Cu$_1$B$_{15}$. All structure states contained a certain portion of crystalline phase in the surface layer, where the penetration profiles $c(x, t)$ were measured. It was observed that the profiles were composed at least of two segments in both cases, which was interpreted as a consequence of diffusion along two diffusion paths with different diffusion coefficients. One of the segments was ascribed to diffusion along interfaces. In the present paper, diffusion of Mo is studied in three alloys Fe$_{79}$Mo$_8$Cu$_1$B$_{12}$ (further referred to as B12), Fe$_{76}$Mo$_8$Cu$_1$B$_{15}$ (B15), and Fe$_{74}$Mo$_8$Cu$_1$B$_{17}$ (B17) that differ in the ratio Fe/B. Before the diffusion measurement, the alloys were crystallized in order to make the "rapid" diffusion path (along the interfaces) extremely expressive. This enables better separation of respective diffusion flux ("short-circuit" diffusion flux) and facilitates the study of Mo diffusion almost exclusively *in* interfaces of Fe$_{79-y}$Mo$_8$Cu$_1$B$_{12+y}$ alloys.

2. Experimental details

Experimental alloys were prepared in Department of Metal Physics, Institute of Physics SAS, Slovakia, by planar flow casting technique as ribbons of about 10 mm wide and about 30 μm thick. Circular diffu-

*Corresponding author: tel.: +420 539 220 422; fax: +420 541 218 657; e-mail address: cermak@ipm.cz
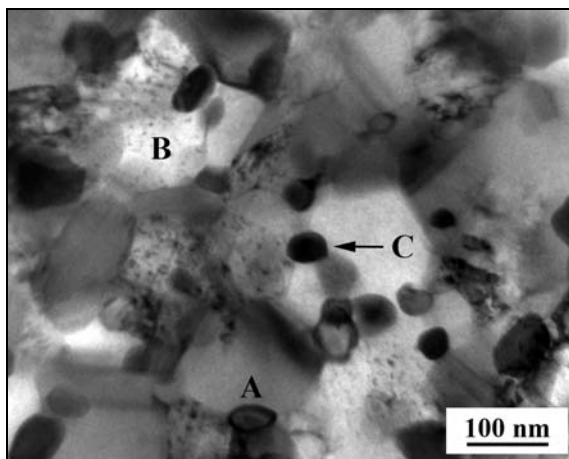
Fig. 1. TEM micrograph of B15. **A:** ratio r = at.% Mo/at.% Fe = 0.02 (mean grain size $d \sim 150$ nm), **B:** $r = 0.09$ ($d \sim 150$ nm) and **C:** $r = 0.83$ ($d \sim 30$ nm).
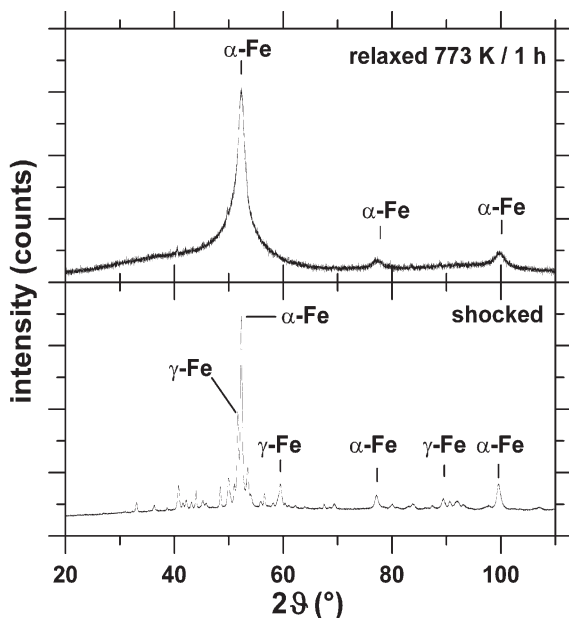

Fig. 2. XRD spectrum measured for B15 alloy in relaxed state and after the severe temperature shock in vacuum.

T a b l e 1. Diffusion coefficients of ^{99}Mo, D_b, *in* GBs of $Fe_{79-y}Mo_8Cu_1B_{12+y}$ alloys calculated from Eq. (2). All values of D_b are in 10^{-17} m^2·s^{-1}, typical relative error of D_b is about $\pm$ 20 pct

T (K)/t (h)	Alloy		
	B12	B15	B17
573/240	0.65	0.42	0.072
623/24	5.6	1.8	1.4
673/1	33	55	15
723/1	110	120	54
773/0.5	280	370	140

rich phase **C**. An attempt was made to identify the alloy components by XRD: It can be seen in the lower part of Fig. 2 that the crystalline phase is formed prevailingly by α-Fe (bcc) (compare with the upper part of Fig. 2 obtained with slightly relaxed only B15 alloy). Moreover, certain portion of γ-Fe (fcc) can be also detected in the shocked alloy. The other peaks are due to boride phase: besides borides $Fe_{23}B_6$ and Fe_3B reported in [1] for differently thermally treated $Fe_{79-y}Mo_8Cu_1B_{12+y}$ alloys, also Mo_2B_5, MoB_2 and Fe_2B may be present in the shocked alloy. With respect to typical ratio r = at.% Mo/at.% Fe = 0.83 obtained for phase **C**, it can be deduced that – in average – Mo prevails Fe in boride phase.

An assessment of mean coherence length (MCL) led to values MCL = (29 $\pm$ 2) nm for boride phase (agrees with the mean size of phase **C** in Fig. 1) and MCL = (15 $\pm$ 2) nm for α-Fe, which is reasonably close to the size of finely dispersed Fe particles in phase **B**.

The shiny (air) side was used for diffusion measurement. Thin radioactive layer of radioisotope ^{99}Mo was deposited by the vacuum evaporation technique (see, e.g., in [9]). After that, the samples were wrapped into envelopes of Ta foil that acted as a getter protecting the sample surface against the rest oxygen and they also protected the extremely brittle samples against mechanical damage. The wrapped samples were sealed in evacuated silica ampoules filled with pure (6N) Ar under pressure of about 0.95 atm. The diffusion anneals were performed in horizontal tube furnaces with temperatures stabilized within $\pm$ 1 K; for the diffusion temperatures T and times t – see Table 1.

The penetration curves $c(x, t)$ (relative concentration of ^{99}Mo in depth x after the diffusion anneal of duration t) were measured by serial sectioning method [10]. The diffusion zone was sectioned by sputtering with accelerated Ar$^+$ ions (accelerating potential: 2 kV) and the co-ordinate x was calculated from the total weight decrement of respective sample (typically: 10^{-1} mg), original sample thickness and sputtering time (6–18 hs). The samples were rotated (about
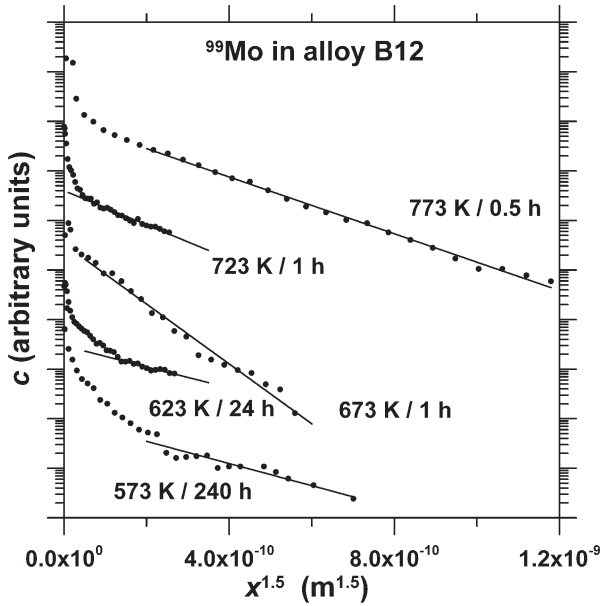
sion samples (diameter 10 mm) were die cut from the ribbons with presser and then subjected to a thermal treatment. The latter consisted in a thermal shock in vacuum (3×10^{-6} mbar). Temperature of the heat source was 1273 K, the distance between the source and samples was 30 mm and the duration of the shock was 10 s. The aim of the thermal treatment was to achieve almost totally crystallized fine-grained structure. It can be seen in Fig. 1 that the structure after the treatment consisted of three distinct components: (*i*) iron-rich phase **A**, (*ii*) the relaxed amorphous phase **B** with fine dispersion in it, and (*iii*) molybdenum-

Fig. 3. Penetration profiles of ^{99}Mo measured in B12 alloy.
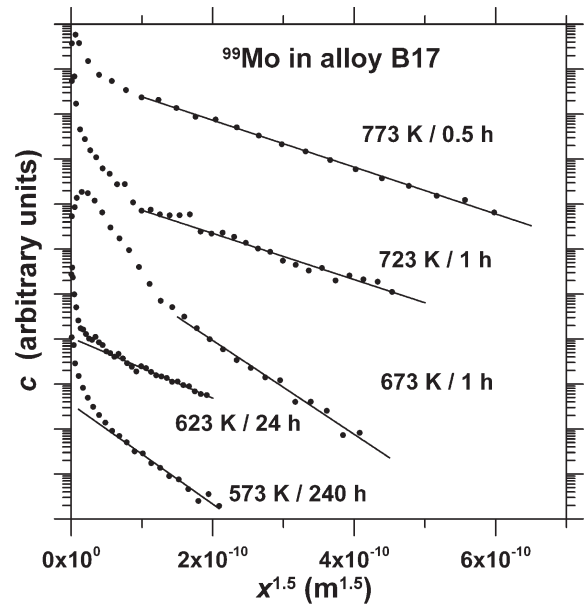

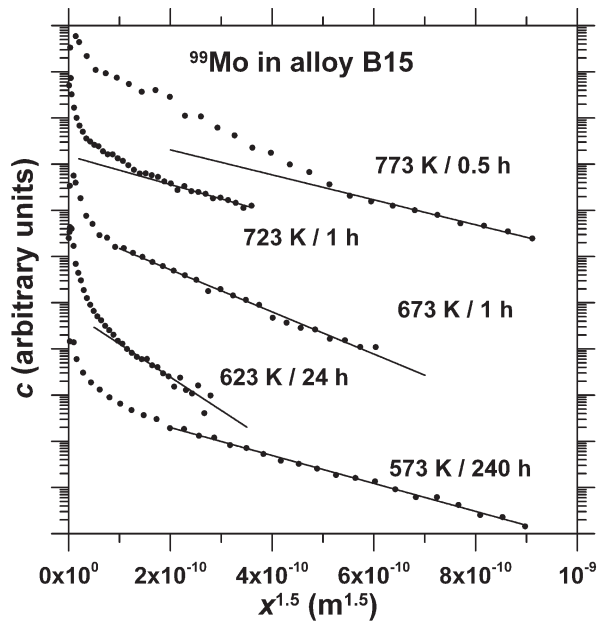Fig. 5. Penetration profiles of ^{99}Mo measured in B17 alloy.

Fig. 4. Penetration profiles of ^{99}Mo measured in B15 alloy.

7 rpm) during the sputtering and the angle between the normal of the sputtered surface and the Ar$^+$ beam was 60°. Such an arrangement was used to eliminate the *knock-on* effect [11, 12].

3. Results and discussion

The primary results are the penetration curves that can be seen in Figs. 3–5. It can be seen that –

after the initial steep part that is due, most likely, to surface effects – the profiles can be considered linear in co-ordinates log c vs. $x^{1.5}$. Such a feature was reported earlier in paper [13] for so-called transition A-B diffusion regime in polycrystals (for the classification of regimes – see, e.g., [14]).

According to authors of ref. [13], A-B regime can be expected when the mean diffusion distance $\alpha = \sqrt{D\,t}$ (D – coefficient of volume diffusion, t – diffusion time) in the bulk adjoining the grain boundary (GB) is comparable with the grain size d:

$$0.3\,\alpha \leq d \leq 4\,\alpha. \qquad (1)$$

In such a case, the authors propose an approximation relation for the self-diffusion coefficient in GBs, D_{b}

$$D_{\mathrm{b}} \cong 16.48\,\frac{D^{0.1}}{\delta^{0.2}\,t^{0.9}}\left(-\frac{\partial \ln c}{\partial x^{1.5}}\right)^{-4/3}, \qquad (2)$$

where δ is the GB width (~ 0.5 nm [14]). Very weak dependence of D_{b} on D and on δ offers two great advantages of the Eq. (2): (i) a rough estimate of D only is sufficient for reasonably accurate assessment of D_{b}, and (ii) the diffusion coefficient *in* the GB, D_{b}, can be estimated. Taking values of D obtained earlier for Mo diffusion in relaxed $Fe_{76}Mo_8Cu_1B_{15}$ [15], $D = (1.2 \times 10^{-5})$ m$^2\cdot$s^{-1} exp $(-165$ kJ$\cdot$mol$^{-1}RT)$, it can be easily shown that $\alpha \sim 100$ nm. This, together with $d \sim 150$ nm (see the mean size of grains **B** in Fig. 1), implies that the relation (1) is fulfilled and, hence, Eq. (2) can be applied. Calculated values are summarized in Table 1.

Ta b l e 2. Arrhenius parameters of ^{99}Mo diffusion in GBs of $\mathrm{Fe}_{79-y}\mathrm{Mo}_8\mathrm{Cu}_1\mathrm{B}_{12+y}$ alloys

y	Alloy	D_{bo} (m$^2\cdot$s^{-1})	Q (kJ$\cdot$mol^{-1})
0	B12	$\left(1.4\,^{+2.1}_{-0.8}\right)\times 10^{-7}$	112.5 ± 5.1
3	B15	$\left(3.7\,^{+58}_{-3.5}\right)\times 10^{-6}$	132 ± 15
5	B17	$\left(6.8\,^{+49}_{-6.0}\right)\times 10^{-6}$	140 ± 12
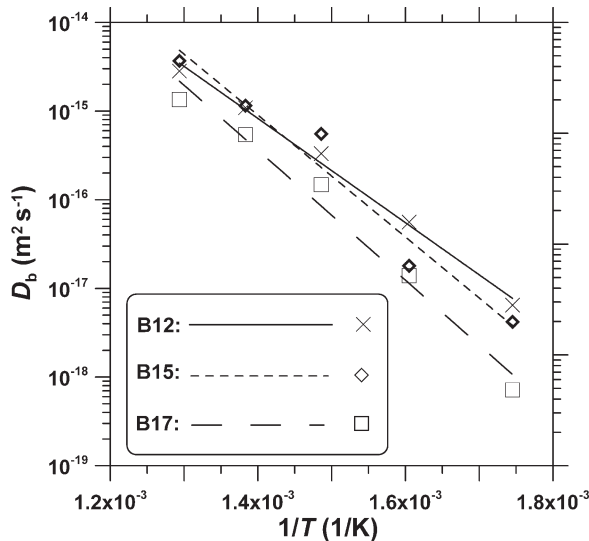
Fig. 6. Temperature dependence of D_{b}.
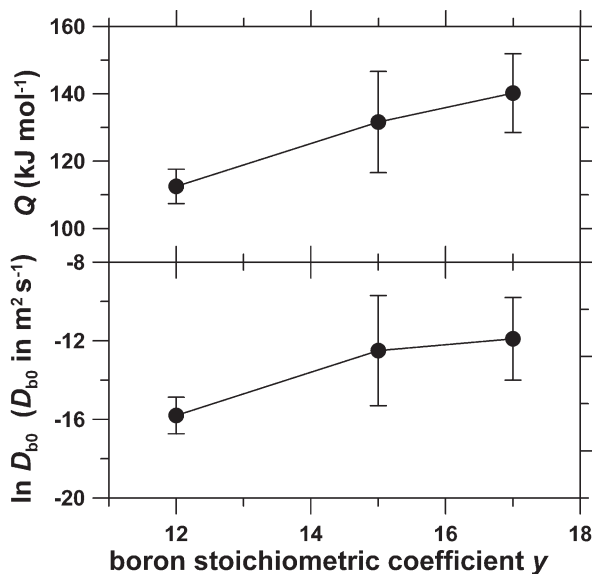
Fig. 7. Arrhenius parameters of D_{b}.

Temperature dependence $D_{\mathrm{b}} = D_{\mathrm{b0}}\exp(-Q/RT)$ is shown in Fig. 6, for Arrhenius parameters (fre-
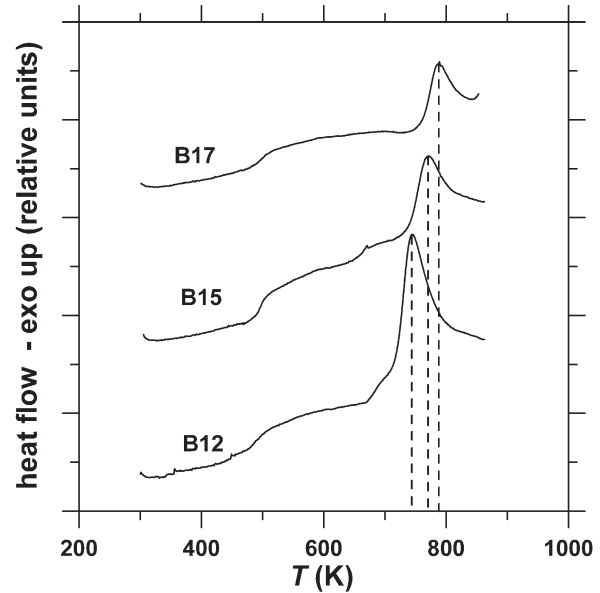
Fig. 8. DSC crystallization curves of $\mathrm{Fe}_{79-y}\mathrm{Mo}_8\mathrm{Cu}_1\mathrm{B}_{12+y}$ alloys (10 K$\cdot$min^{-1}).

quency factor D_{b0} and activation enthalpy Q) – see Table 2 and Fig. 7.

Taking into account the shape of penetration curves (linearity of "tails" in co-ordinates $\ln c$ vs. $x^{1.5}$), it was concluded that the observed Mo diffusion occurs prevailingly along the GBs round the relaxed amorphous phase (**B** in Fig. 1) in the A-B kinetics. Diffusion in growing Fe crystallites and the leakage of diffusing Mo atoms from GBs in their interiors can be excluded due to very low Mo diffusivity in Fe reported, e.g., in [16].

It can be deduced that Mo diffusion in boride phase is also not too fast, since with increasing y the Mo diffusion coefficients decrease (Fig. 6) and activation enthalpy Q increases (Fig. 7). This is in a qualitative agreement with increasing crystallization temperatures (see DSC curves in Fig. 8) with increasing y, since the crystallization temperature scales the easiness of structure transformation.

4. Conclusions

Observed variation of Mo diffusion coefficient and crystallization temperature with y enables to sketch out the likely mechanism of structure transformation: the Mo is expelled from the growing Fe crystallites (**A** in Fig. 1) and diffuses along the reaction front (characterized by D_{b}) to boride nuclei at GBs to build the precipitates (**C** in Fig. 1). Mo is trapped in borides, which slows down its diffusion coefficient D_{b} and raises the activation enthalpy of Mo diffusion, Q. Effectiveness of retardation of Mo diffusivity increases with

increasing y and, also, the pinning effect of borides at GBs raises effectively the crystallization temperature (Fig. 8).

Acknowledgements

References

[1] ANDIĆ, Z.—KORAĆ, M.—TASIĆ, M.—RAIĆ, K.—KAMBEROVIĆ, Ž.: Kovove Mater., *44*, 2006, p. 145.
[2] ROUPCOVÁ, P.—SCHNEEWEISS, O.—BEZDIČ-KA, P.—PETROVIČ, P.: Kovove Mater., *44*, 2006, p. 127.
[3] IŽDINSKÝ, K.—IŽDINSKÁ, Z.—DUFEK, J.—IVAN, J.—ZEMÁNKOVÁ, M.: Kovove Mater., *41*, 2003, p. 106.
[4] ĎURIŠIN, J.—ĎURIŠINOVÁ, K.—OROLÍNOVÁ, M.—KATANA, V.: Kovove Mater., *41*, 2003, p. 63.
[5] BESTERCI, M.—KVAČKAJ, T.—KOVÁČ, L.—SÜLLEIOVÁ, K.: Kovove Mater., *44*, 2006, p. 101.
[6] ČERMÁK, J.—STLOUKAL, I.: Kovove Mater., *43*, 2005, p. 338.
[7] SZYMURA, S.—LUKIN, A. A.—BALA, H.—URAWSKA, A.: Kovove Mater., *42*, 2004, p. 375.
[8] ILLEKOVÁ, E.—JANIČKOVIČ, D.—MIGLIERINI, M.—ŠKORVÁNEK, I.: J. Magn. Magn. Mater., *304*, 2006, p. e636.
[9] ČERMÁK, J.—ROTHOVÁ, V.: Intermetallics, *10*, 2002, p. 765.
[10] ADDA, A.—PHILIBERT, J.: La Diffusion dans les Solides. Paris, Saclay, Presses Universitaires de France 1966.
[11] HOFMANN, S.: Rep. Prog. Phys., *61*, 1998, p. 827.
[12] HERTH, S.—EGGERSMANN, M.—EVERSHEIM, P.-D.—WÜRSCHUM, R.: J. Appl. Phys., *95*, 2004, p. 5075.
[13] DIVINSKI, S. V.—HISKER, F.—KANG, Y.-S.—LEE, J.-S.—HERZIG, CH.: Interface Sci., *11*, 2003, p. 67.
[14] KAUR, I.—GUST, W.: Fundamentals of Grain and Interphase Boundary Diffusion. Stuttgart, Ziegler Press 1988.
[15] ČERMÁK, J.—STLOUKAL, I.: Phys. Stat. Sol. (a), *203*, 2006, p. 2386.
[16] NITTA, H.—YAMAMOTO, T.—KANO, R.—TAKASAWA, K.—IIDA, T.—YAMAZAKI, Y.—OGU, S.—IIJIMA, Y.: Acta Mater., *50*, 2002, p. 4117.